# Origin of the magnetic properties of Fe-implanted 4H-SiC semiconductor

Lindor Diallo, Abdeslem Fnidiki, Luc Lechevallier, Jean Juraszek, Michel Viret, Marc Marteau, Dominique Eyidi, Alain Declémy

Journal of Applied Physics

# Origin of the magnetic properties of Fe-implanted 4H-SiC semiconductor

Cite as: J. Appl. Phys. **127**, 183901 (2020); https://doi.org/10.1063/5.0005061
Submitted: 25 February 2020 . Accepted: 17 April 2020 . Published Online: 08 May 2020

L. Diallo, A. Fnidiki, L. Lechevallier, J. Juraszek, M. Viret, M. Marteau, D. Eyidi, and A. Declémy



AIP Publishing

Journal of Applied Physics ARTICLE scitation.org/journal/jap

# Origin of the magnetic properties of Fe-implanted 4H-SiC semiconductor

Cite as: J. Appl. Phys. **127**, 183901 (2020); doi: 10.1063/5.0005061
Submitted: 25 February 2020 · Accepted: 17 April 2020 ·
Published Online: 8 May 2020



L. Diallo,[1] A. Fnidiki,[1,a)] L. Lechevallier,[1,2] J. Juraszek,[1] M. Viret,[3] M. Marteau, D. Eyidi, and A. Declémy

## AFFILIATIONS

[1]Normandie University, UNIROUEN, INSA Rouen, CNRS, GPM, 76000 Rouen, France
[2]Département de GEII, Université de Cergy-Pontoise, rue d'Eragny, Neuville sur Oise, 95031 Cergy-Pontoise, France
[3]Service de Physique de l'Etat Condensé (DSM/IRAMIS/SPEC), UMR 3680 CNRS, Bât. 772, Orme des Merisiers, CEA Saclay, 91191 Gif sur Yvette, France
[4]Institut PPRIME, UPR 3346 CNRS, Université de Poitiers, ENSMA, SP2MI, téléport 2, 11 Bvd M. et P. Curie, 86962 Futuroscope, Chasseneuil, France

[a)]**Author to whom correspondence should be addressed:** abdeslem.fnidiki@univ-rouen.fr

## ABSTRACT

p-doped 4H-SiC substrates were implanted with $^{57}$Fe ions at energies ranging from 30 to 160 keV and subjected to a rapid thermal annealing in order to produce a homogeneous Fe concentration inside a 100 nm-thick region in the semiconducting SiC material. Using $^{57}$Fe Conversion Electron Mössbauer Spectrometry and Superconducting Quantum Interference Device magnetometry, we give evidence that the ferromagnetism obtained in SiC implanted with a $^{57}$Fe atoms concentration close to 2% is not only due to the formation of some Fe–Si magnetic nanoparticles but also originates from magnetic Fe atoms diluted in the matrix of the semiconductor. So, values of Fe atoms magnetizations contained in nanoparticles and Fe atoms diluted in the matrix and the Curie temperatures associated with the nanoparticles and to the matrix have been determined.



## I. INTRODUCTION

In the spintronics research domain, the use of devices containing materials which rely the charge and spin properties of the carriers is of prime interest. Among these materials, the diluted magnetic semiconductors (DMSs) were the subject of numerous studies in the two last decades. They use a semiconductor matrix doped or implanted with a 3D magnetic element (Cr, Mn, Fe, and Co). This allows keeping the semiconductor nature of the material but also providing it ferromagnetic (FM) properties. The discovery of DMSs with relatively high Curie temperatures ($T_C$), such as (In, Mn) As[1] and (Ga, Mn) As[2] initiated important researches over many years in order to understand the origin of the magnetic properties involved in these materials and to obtain $T_C$ higher than the room temperature (RT). Many experimental works about the growth and the annealing of these materials have been made in order to minimize the presence of secondary phases, which are detrimental to the desired properties. A possibility to obtain $T_C$ values higher than RT was considered for wide-gap DMSs with a high concentration of free holes.[3] This revived the study of these materials and led to new experiments toward the discovery of new DMSs with high $T_C$.

Many authors reported the observation of ferromagnetism in DMSs above RT. However, in most cases, the ferromagnetism observed is the consequence of the presence of magnetic particles in their samples, composed of phases based on transition metal (TM).[4] These experimental studies stimulated theoretical works some of which have shown the FM ordering can be partly explained from the exchange interaction between charge carriers and doping magnetic ions.[5] But, despite intense research studies, no $T_C$ higher than RT has now been obtained in DMSs. Moreover, the nature and origin of ferromagnetism in these materials remain controversial.[6] Silicon carbide (SiC) is a wide bandgap semiconductor, which has been considered as a possible candidate for spin electronics applications. SiC is a well-known semiconductor in the industry for many years. It has been developed and commercialized for these numerous applications in the high frequency and high-power domains.

Ferromagnetism has been observed in 4H-SiC doped with Ni, Mn, and Fe TM atoms with $T_C$ values varying from below to close to RT; the authors attribute the magnetism to a DMS behavior.[7,8] According to Dupeyrat *et al.* and Diallo *et al.*,[9,10] the presence of magnetic particles mainly containing the $Fe_3Si$ phase is mainly responsible for the magnetic properties observed in a 6H-SiC system implanted with a 6% concentration of Fe atoms and annealed at high temperatures (>900 °C). However, for Song *et al.*,[11] the presence of $Fe_3Si$ is not responsible of FM order in Fe-doped SiC and Fe traces in SiC are sufficient to induce a high temperature FM arrangement. In another paper of Song *et al.*[12] dealing with Mn atom in 4H-SiC, the FM order was obtained at around 250 K for a low Mn concentration ($10^{-4}$ molar fraction). These authors showed that defect-related effects played a more important role in the magnetic order obtained in these samples than the Mn content. Liu *et al.* also evidenced ferromagnetism in 4H-SiC after neutron irradiation.[13]

Theoretical studies using *ab initio* calculations were used to investigate the magnetic properties of SiC implanted with TM. According to the structural configuration of the substitution site, Fe was found non-magnetic or magnetic, while Cr and Mn were found to be magnetic at a substitutional Si site.[5,14,15] The researchers found that the Si sites were more favorable compared to the C-sites for Fe substitution and the appearance of magnetism.[5,14,18] Recently, Los *et al.*[5] also reported that Fe in SiC could exist in both magnetic and non-magnetic states, which depend on the Fe atom environment in the host matrix. The theoretical works of Los *et al.*[5,28] showed by *ab initio* calculations that the FM order is established for the Si substitution by Fe in the (Si/4C) tetrahedron. In hexagonal SiC, the ferromagnetism would be due to an increase of the Fe–C length along the c direction of this tetrahedron, the electronic structure of the Fe atoms being strongly affected by the neighboring of the C atoms. A mean value of the magnetic moment going from 2.95 to 3.1 $\mu_B$ (Bohr magneton) has been reported as the result of the increase in the Fe–C length along the c axis.[5] This Fe–C length increase has been also evidenced experimentally by Dupeyrat *et al.*[9] in 2 at. % Fe implanted 6H-SiC, for which a strong diffraction streak along the surface normal direction was ascribed to a tensile strain gradient along the c axis in the implanted part of the crystal.

In recent communications,[10,16,17] we reported that the ferromagnetism observed in 6H-SiC implanted with 4–6 at. % Fe are mainly due to Fe-rich magnetic nanoparticles ($Fe_3Si$, $Fe_2Si$, $Fe_5Si_3$, and FeSi phases), but also to Fe-implanted atoms diluted in the SiC matrix, located in substitutional Si-sites. The structural studies of Atom Probe Tomography (APT) revealed a random distribution of Fe atoms in the SiC matrix into the 2 at. % Fe as-implanted sample and the presence of Fe-rich nanoparticles in the annealed samples. The investigation of the same samples by $^{57}$Fe conversion electron Mössbauer spectrometry (CEMS) showed that at least 35% of the implanted Fe atoms are located at substitutional sites in the 1300 °C annealed sample.

In this paper, we study the magnetic properties evidenced in p-type 4H-SiC samples implanted with Fe low doses (2 at. %). In contrast with the 6H-SiC samples implanted with 6% of Fe atoms, we show by Mössbauer spectrometry that the nanoparticles do not contain the $Fe_3Si$ phase (up to the 1300 °C annealing), which is mainly responsible of the magnetism of the samples implanted with 6 Fe at. % and annealed at 1300 °C. Thanks to a SQUID magnetometer, we determine by a fit procedure of the temperature dependence of the saturation magnetization the values of magnetizations of Fe atoms contained in nanoparticles and diluted in the matrix and the Curie temperatures associated with the nanoparticles and with the matrix.

## II. EXPERIMENTAL METHODOLOGY

4H-SiC substrates (0001-oriented) from commercial wafers (CREE) with a 200 nm-thick uppermost p-type epitaxial layer ($n_A - n_D \sim 10^{+19}$ cm$^{-3}$) were implanted with 30–160 keV $^{57}Fe^+$ ions. The implanted fluence of $2 \times 10^{+16}$/cm$^2$ leads to an Fe concentration of about 2 at. % inside a region at a depth going from 20 nm to 100 nm of the sample surface. This composition was checked by Rutherford backscattering spectrometry (RBS) at the CSNSM-Orsay (Centre de Sciences Nucléaires et de Sciences de la Matière).[9] The samples were held at 550 °C during implantation in order to avoid amorphzation.[19] After implantation, samples were subjected to a rapid thermal annealing at 900 °C, 1100 °C, and 1300 °C for 4 min, respectively.

The CEMS technique has a penetration depth of about 80–100 nm compared to the overall thickness of the sample (400 $\mu$m) and is useful for analyzing the near surface region[20,21] of the implanted samples studied in this work. CEMS experiments were performed at RT by using a $^{57}$Co source in a rhodium matrix in a constant acceleration mode. Magnetic CEMS spectra were fitted with a discrete distribution of hyperfine fields ($B_{hf}$) with a least-squares procedure.[22] A correlation between hyperfine field and isomer shift (δ) was used to take into account the Fe environment distribution.[23,24] Paramagnetic spectra are fitted with a discrete distribution of quadrupole splitting (QS). A correlation between QS and δ was also employed for asymmetrical spectra.[25] δ values at the $^{57}$Fe nuclei are given relative to α-Fe at RT. Estimated errors for the hyperfine parameters originate from the statistical errors σ given by the fitting program, taking 3 σ.

Magnetic properties have been also studied by means of a Superconducting Quantum Interference Device (SQUID) magnetometer at 10 K and 300 K with the applied field up to 1.5 T in the plane of the sample surface. Thermal saturation magnetization has been measured at 0.5 T between 4 K and 400 K.

## III. RESULTS AND DISCUSSION

### A. Mössbauer spectrometry

The Mössbauer spectra of the as-implanted and annealed samples at 900 and 1100 °C are shown in Fig. 1. All the spectra exhibit an asymmetric paramagnetic doublet and have been fitted with a quadrupolar splitting distribution P(QS). Each iron environment has a quadrupole effect with an isomer shift different from other iron environments. This effect explains the raison using a correlation between the isomer shift and the quadrupole effect.

For the as-implanted specimen [Fig. 1(a)], P(QS) has a Gaussian shape with a mean value of $\langle QS \rangle = 1.17$ mm/s. The spread of the distribution indicates that the environments of the Fe implanted atoms are distributed, in agreement with amorphous or

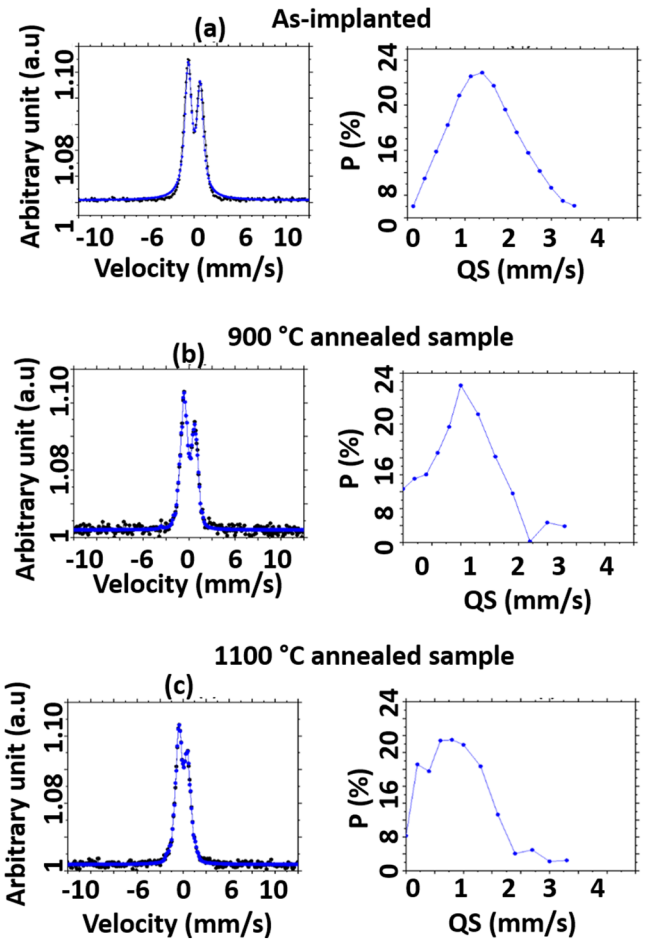


**FIG. 1.** $^{57}$Fe Mössbauer spectra at RT and corresponding quadrupole splitting distributions of the 2 at. % Fe-implanted sample (a) and 4 min annealed samples at 900 °C (b) and 1100 °C (c).

strongly damaged regions produced inside the SiC matrix. After annealing at 900 °C, the shape of the Mössbauer spectrum and P (QS) [Fig. 1(b)] is narrower and the average value of the quadrupole splitting is reduced ($\langle QS \rangle = 0.98$ mm/s). This result can be explained by a restructuring of the SiC–Fe matrix and a recombination of the defects caused by the implantation. The shape of the spectrum of the 1100 °C annealed sample [Fig. 2(c)] is close to that of the 900 °C annealed sample; therefore, similar effects are expected for these two annealing temperatures. Table I gives the hyperfine parameters deduced from the fit of the three samples. In the as-implanted state, the average value of $\langle \delta \rangle = 0.23$ mm/s indicates a 3+ oxidation state of Fe atoms. It can be seen from Table I that the mean isomer shift value of the as implanted sample and 900 and 1100 °C annealed samples decreases when the annealing temperature increases. This $\langle \delta \rangle$ value as well as the $\langle QS \rangle$ value are very close to the values obtained in Refs. 8 and 26. After annealing at 900 and 1100 °C, the $\langle \delta \rangle$ average values are 0.12 mm/s and

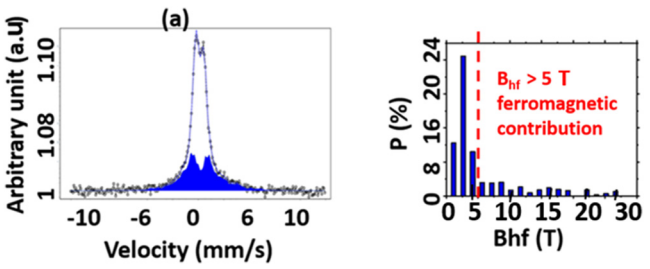


**FIG. 2.** $^{57}$Fe Mössbauer spectrum at RT and corresponding hyperfine field distribution of the 2 at. % Fe-implanted sample after annealing at 1300 °C, blue contribution corresponds to ferromagnetic contribution.

0.11 mm/s, respectively, still indicating a 3+ oxidation state of Fe atoms.

Figure 2 displays the Mössbauer spectrum of the implanted sample annealed at 1300 °C. The spectrum is composed of an asymmetric quadrupolar doublet and an additional broad magnetic component. This broad magnetic component is characteristic of FM interactions. The spectrum has been fitted with a distribution of hyperfine fields $P(B_{hf})$ extending to 27 T. Considering that the $B_{hf}$, greater than 5 T, come from the FM Fe atoms, the proportion of FM Fe atoms can then be estimated at about 32% with respect to the total amount of implanted Fe atoms. From the hyperfine distributions analysis, we obtained the average hyperfine field calculated from the whole distribution as $\langle B_{hf} \rangle = 5.8$ T and the average values of isomer shift $\langle \delta \rangle = 0.192$ mm/s, and these values are $\langle B_{hf} \rangle_{ferro} = 18.2$ T and to $\langle \delta \rangle_{ferro} = 0.04$ mm/s, when considering that only the high values of hyperfine fields above 5 T come from ferromagnetic iron [the paramagnetic component ($B_{hf} < 5$ T) is not taken into account]. We can observe that this sample does not evidence the existence of two hyperfine fields (for 20 and 31 T) which are characteristic of the presence of the $DO_3$ structure in the $Fe_3Si$ phase. In the samples implanted with 6% of Fe atoms, this phase is contained in the biggest nanoparticles and is mostly responsible for the magnetism of these samples.[10] Consequently, these new samples do not contain the $Fe_3Si$ phase which is not responsible for the magnetism of this sample.

As we can see here, the magnetic properties of this sample are the sum of the two contributions, a paramagnetic or super paramagnetic (asymmetric doublet) contribution, which represents 67% of the total surface of the spectrum and a ferromagnetic contribution (very wide sextuplet at the base of the spectrum), which

**TABLE I.** Summary of the average values of quadrupole splitting $\langle QS \rangle$ and isomer shift $\langle \delta \rangle$ deduced from the Mössbauer spectra of the as-implanted and annealed samples.

| Sample | $\langle QS \rangle$ (mm/s) | $\langle \delta \rangle$ (mm/s) |
|---|---|---|
| As-implanted | 1.17 | 0.23 |
| Annealed at 900 °C | 0.98 | 0.12 |
| Annealed at 1100 °C | 0.86 | 0.11 |

represents 33%. The presence of an asymmetric doublet can be explained by the low concentration of Fe, where most of the Fe atoms are contained in the nanoparticles.

This Mössbauer spectrum can then be analyzed with the Gunnlaugsson model[27] leading to two singlet (paramagnetic) components: $Fe_S$ (Fe-substituted atoms in the SiC matrix, preferentially at Si-sites as recalled above) = 35% and $Fe_{i,C}$ = 33%, and a sextuplet (FM) component Fe(ferro) = 32%, exactly as the above decomposition with the hyperfine field distribution. The Gunnlaugsson model concerns only the para-magnetic or super paramagnetic contribution (asymmetric doublet) and makes it possible to take into account the different environments around the atoms of $^{57}$Fe in low concentration (diluted) 2% in SiC and to follow the evolution of the location of these atoms of $^{57}$Fe diluted in the crystal structure of SiC.

In addition, the APT results for the annealed sample at 1300 °C show that 40% of the Fe atoms are diluted in the SiC matrix, while the remaining 60% being in Fe-rich nanoparticles.[34] From the 1300 °C annealed sample, the nanoparticle's size range from 1 to 9 nm. However, these nanoparticles have in their core a rich phase such as the $FeSi_2$, FeSi, $Fe_5Si_3$ $Fe_2Si$, and $Fe_3Si$ phase. The measuring size method and core phase determination are published in the works of Diallo *et al.*[17,34] From these results, it can be estimated that there is ∼40%–35% ∼ 5% Fe atoms diluted at interstitial positions in the SiC matrix and ∼60%–32% ∼ 28% Fe atoms at non-magnetic sites inside nanoparticles. These two species correspond to the $Fe_{i,C}$ (paramagnetic) component ∼33% in the Gunnlaugsson model.

These results will be useful in the section dealing with magnetization measurements as a function of temperature performed in SQUID, which will be seen later on.

## B. SQUID magnetometry

Figure 3 shows the magnetization loops for a sample implanted at 550 °C and annealed at 1300 °C measured at 10 K (a) and 300 K (b). The diamagnetic signal of the bulk SiC sample was subtracted from all the measurements. No magnetic signal was detected for the as-implanted sample at 550 °C. The M (H) curves obtained for the annealed samples at 900, 1100, and 1300 °C show a hysteresis effect at 10 K with a non-zero coercive field. Only the obtained results of 1300 °C sample are shown here. At 300 K, the annealed sample exhibits a saturation magnetization, and a coercive field practically equal to zero [or difficult to measure, Fig. 3, inset on (b)]. This type of behavior is characteristic of a superparamagnetic behavior due to the existence of nanoparticles (incidentally visible in APT[17]). In Mössbauer spectrometry, the sample annealed at 1300 °C appears magnetic at 300 K.

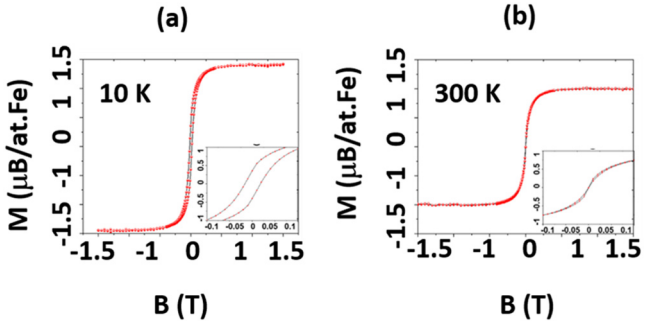


**FIG. 3.** Magnetic hysteresis loops at 10 K (a) and 300 K (b) for 2 at. % Fe-implanted sample after annealing at 1300 °C. The insets show a zoom in the low magnetic field region.

In order to characterize the magnetic behavior of the 1300 °C annealed sample, the temperature dependence of the saturation magnetization $M_s$ was measured under an applied field of 0.5 T. The experimental curve $M_s(T)$ can be seen as the red curve in Fig. 4. This figure underlines the unconventional non-Brillouin-function like character of the magnetization curve. As mentioned above, the magnetization of the annealed sample is the sum of the magnetic Si-substituted Fe diluted atoms contribution and the Fe-rich nanoparticles contribution. The temperature dependence of saturation magnetization of Fe-rich nanoparticles $M_{nanop}(T)$ can be described by the following relation:

$$M_{nanop}(T) = M_{nanop}\left(1 - \frac{T}{Tc_{nanop}}\right)^{0.36}, \quad (1)$$

where 0.36 is the Heisenberg nanocrystal line ferromagnet's critical exponent,[29,30] $M_{nanop}$ the mean value of the saturation magnetization of nanoparticles at 0 K and $Tc_{nanop}$ the Curie temperature for the nanoparticles.

Following this, the experimental curve of Fig. 4 can be well described by the following relation:

$$M_s(T) = M_{nanop}\left(1 - \frac{T}{Tc_{nanop}}\right)^{0.36} + M_{dilu}\left(1 - \frac{T}{Tc_{dilu}}\right). \quad (2)$$

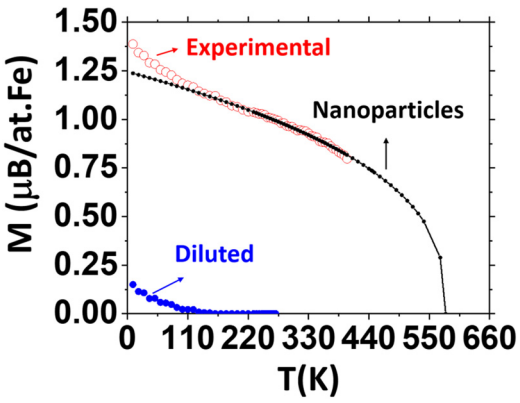


**FIG. 4.** Temperature dependence of the saturation magnetization $M_s$ for the 2 at. % Fe-implanted sample after annealing at 1300 °C. A magnetic field of 0.5 T was applied during measurement. Red dots: experimental data. Black curve: fit of the experimental data using Eq. (2) (contribution of the FeSi nanoparticles). The corresponding contribution from the diluted Fe atoms inside the matrix is plotted as blue dots.

The linear law $M_{diluted}\left(1-\frac{T}{Tc_{dilu}}\right)$ due to Fe diluted atoms has been introduced in the Bouzerrar works to calculate the magnetization of samples containing small contents of TM atoms in semiconductors.[31] $M_{dilu}$ and $Tc_{dilu}$ are related to magnetic Si-substituted Fe diluted atoms. The fit procedure is represented in Fig. 4 by the black line for nanoparticles. The fit procedure allows also determining the temperature dependence of the spontaneous magnetization of diluted Fe atoms. The blue curve corresponding to this last one is obtained by making the difference between experimental curve (red curve) and fitting curve for nanoparticles (black line).

It can be noted that such a linear behavior (between 30 and 150 K) of the magnetization of magnetic contribution of the diluted atoms has been observed in InMnP[31] with $T_C$ in the 23–43 K range for 2.5–5 at. % Mn concentration in InP. The authors make the connection of this kind of behavior with "the Fermi level lying in a well-defined impurity band whose is not totally separated from the valence band." This is the case in DOS calculations of Los *et al.*[5] for 4 at. % Si-substituted Fe-atoms in 4H-SiC.

The fit procedure of the temperature dependence allows determining the saturation magnetization and the Curie temperatures, respectively, associated with the Fe atoms contained in the nanoparticles and the Fe atoms diluted in the matrix. Thus, we obtained $M_{nanop} \sim 1.245\,\mu_B$/at. Fe, $M_{dilu} \sim 0.14\,\mu_B$/at. Fe, $Tc_{nanop} \sim 580$ K, and $Tc_{dilu} \sim 120$ K.

This calculation shows that the Fe diluted atoms are not ferromagnetic at 300 K, and thus do not contribute to the FM part of the Mössbauer spectrum at 300 K, which is only due to Fe-rich nanoparticles.

The Curie temperature of nanoparticles is 580 K. The value is very close to these observed in silicides $Fe_5Si_3$ or $Fe_2Si$.[32,33] As observed in the Atom Probe Tomography results published in the works of Diallo *et al.*,[34] 60% Fe atoms are contained in the nanoparticles and most of them are $Fe_2Si$ and $Fe_5Si_3$ rich Fe phases. In comparison with the 900 °C annealed sample,[34] this Tc is reasonable for the expected composition and size of the particles.

Considering the $Fe_S$ (Fe diluted atoms substituted at Si-sites) value (35%) obtained from Mössbauer spectrometry for the 1300 °C annealed sample, the mean value of the magnetic moment of Fe diluted atoms substituted at Si-sites can be estimated as being $\sim 0.14/0.35 \sim 0.4\,\mu_B$. Considering that APT has shown that ~60% of the Fe atoms are located in Fe-rich nanoparticles, the mean value of the magnetic moment of Fe in Fe-rich nanoparticles can be estimated as $M_{nanop} \sim 1.245/0.6 \sim 2.0\,\mu_B$.

## IV. CONCLUSION

2 at. % Fe-implanted 4H-SiC samples annealed at different temperatures have been investigated by Mössbauer spectrometry and SQUID magnetometry. It is found paramagnetic behavior in the as implanted sample and superparamagnetic in the 900 and 1100 °C annealed samples. The effect is due to Fe–Si nanoparticles, introduced by thermal treatment. The decrease of mean value of the quadrupole splitting from as implanted to annealing sample is mainly due to a restructuring of the SiC–Fe matrix and the recombination of the defects caused by the implantation. It was found that the oxidation state of Fe in the as-implanted state is therefore ⟨3+⟩, which reflects a low spin state and a high degree of valence, as well as after annealing at 900 and 1100 °C. Oppositely, the 1300 °C annealed sample is FM. The temperature dependence of the saturation magnetization of this sample is interpreted as a result from a contribution due to the presence of Fe-rich nanoparticles and a contribution due to magnetic Fe atoms diluted inside the SiC matrix. From the fit, the critical temperatures for magnetic ordering of the nanoparticles and diluted Fe atoms are found to be 580 K and 120 K, respectively. Consequently, the ferromagnetism of this sample is due to slow temperature (below 120 K) to both magnetic diluted Fe atoms and magnetic Fe atoms contained in the Fe-rich nanoparticles while for high temperatures (above 120 K), it is only due to magnetic Fe atoms contained in the Fe-rich nanoparticles. The experimental results presented here unambiguously demonstrate that magnetic Fe diluted atoms play an important role in FM ordering in Fe-implanted SiC with a noticeably high critical temperature (~120 K). This is therefore very promising in the goal of obtaining a DMS at room temperature in Fe implanted SiC.

Using $^{57}$Fe Mössbauer spectrometry and SQUID magnetometry, we show that the magnetic behavior originates not only from the contribution of nanoparticles containing Fe, but also of the Fe diluted atoms inside the semiconducting SiC matrix.

## ACKNOWLEDGMENTS

Region of Normandy and the European Regional Development Fund of Normandy (ERDF) in the frame of the MAGMA project funded this work.

## DATA AVAILABILITY

The data that support the findings of this study are available within the article.

## REFERENCES

[1]H. Munekata, H. Ohno, S. von Molnar, A. Segmüller, L. L. Chang, and L. Esaki, Phys. Rev. Lett. **63**, 1849 (1989).
[2]H. Ohno, A. Shen, F. Matsukura, A. Oiwa, A. Endo, S. Katsumoto, and Y. Iye, Appl. Phys. Lett. **69**, 363 (1996).
[3]T. Dietl, H. Ohno, and F. Matsukura, Phys. Rev. B **63**, 195205 (2001); arxiv.org/abs/cond-mat/0007190v2.
[4]A. Bonanni and T. Dietl, Chem. Soc. Rev. **39**, 528 (2010).
[5]A. V. Los, A. N. Timoshevskii, V. F. Los, and S. A. Kalkuta, Phys. Rev. B **76**, 165204 (2007).
[6]G. Bouzerar and R. Bouzerar, C. R. Phys. **16**, 731 (2015).
[7]N. Theodoropoulou, A. F. Hebard, S. N. G. Chu, M. E. Overberg, C. R. Abernathy, S. J. Pearton, R. G. Wilson, and J. M. Zavada, Electrochem. Solid-State Lett. **4**, G119 (2001).
[8]F. Stromberg, W. Keune, X. Chen, S. Bedanta, H. Reuther, and A. Mücklich, J. Phys. Condens. Matter **18**, 9881 (2006).
[9]C. Dupeyrat, A. Declémy, M. Drouet, D. Eyidi, L. Thomé, A. Debelle, M. Viret, and F. Ott, Phys. B **404**, 4731 (2009).
[10]M. L. Diallo, L. Lechevallier, A. Fnidiki, R. Lardé, A. Debelle, L. Thomé, M. Viret, M. Marteau, D. Eyidi, A. Declémy, F. Cuvilly, and I. Blum, J. Appl. Phys. **117**, 183907 (2015).
[11]B. Song, J. K. Jian, H. Li, M. Lei, H. Q. Bao, X. L. Chen, and G. Wang, Phys. B **403**, 2897 (2008).
[12]B. Song, H. Bao, H. Li, M. Lei, J. Jian, J. Han, X. Zhang, S. Meng, W. Wang, and X. Chen, Appl. Phys. Lett. **94**, 102508 (2009).

[13]Y. Liu, G. Wang, S. Wang, J. Yang, L. Chen, X. Qin, B. Song, B. Wang, and X. Chen, Phys. Rev. Lett. **106**, 087205 (2011).
[14]V. A. Gubanov, C. Boekema, and C. Y. Fong, Appl. Phys. Lett. **78**, 216 (2001).
[15]Y.-S. Kim, Y.-C. Chung, and S.-C. Yi, Mater. Sci. Eng.: B **126**, 194 (2006).
[16]M. L. Diallo, L. Diallo, A. Fnidiki, L. Lechevallier, F. Cuvilly, I. Blum, M. Viret, M. Marteau, D. Eyidi, J. Juraszek, and A. Declémy, J. Appl. Phys. **122**, 083905 (2017).
[17]L. Diallo, A. Fnidiki, L. Lechevallier, A. Zarefy, J. Juraszek, F. Cuvilly, I. Blum, M. Viret, M. Marteau, D. Eyidi, and A. Declemy, IEEE Magn. Lett. **9**, 1–3 (2018).
[18]M. S. Miao and W. R. L. Lambrecht, Phys. Rev. B **68**, 125204 (2003).
[19]W. J. Weber, L. M. Wang, N. Yu, and N. J. Hess, Mater. Sci. Eng.: A **253**, 62 (1998).
[20]F. Richomme, A. Fnidiki, J. Teillet, and M. Toulemonde, Nucl. Instrum. Methods Phys. Res. Sect. B **107**, 374 (1996).
[21]J. P. Eymery, A. Fnidiki, and J. P. Riviere, Nucl. Instrum. Methods Phys. Res. **209-210**, 919 (1983).
[22]A. Fnidiki, F. Richomme, J. Teillet, F. Pierre, P. Boher, and P. Houdy, J. Magn. Magn. Mater. **121**, 520 (1993).
[23]K. M. Hamasha, I. A. Al-Omari, and S. H. Mahmood, Physica B **321**, 154 (2002).
[24]A. Fnidiki, C. Lemoine, and J. Teillet, Physica B **357**, 319 (2005).
[25]J. Teillet, A. Fnidiki, F. Richomme, P. Boher, and P. Houdy, J. Magn. Magn. Mater. **123**, 359 (1993).
[26]C. J. McHargue, A. Perez, and J. C. McCallum, Nucl. Instrum. Methods Phys. Res. Sect. B **59–60**, 1362 (1991).
[27]H. P. Gunnlaugsson, T. E. Mølholt, R. Mantovan, H. Masenda, D. Naidoo, W. B. Dlamini, R. Sielemann, K. Bharuth-Ram, G. Weyer, K. Johnston, G. Langouche, S. Ólafsson, H. P. Gíslason, Y. Kobayashi, Y. Yoshida, M. Fanciulli, and ISOLDE Collaboration, Appl. Phys. Lett. **97**, 142501 (2010).
[28]A. Los and V. Los, J. Phys. Condens. Matter **21**, 206004 (2009).
[29]G. Herzer, IEEE Trans. Magn. **25**, 3327 (1989).
[30]A. Ślawska-Waniewska, M. Gutowski, H. K. Lachowicz, T. Kulik, and H. Matyja, Phys. Rev. B **46**, 14594 (1992).
[31]R. Bouzerar, D. May, U. Löw, D. Machon, P. Melinon, S. Zhou, and G. Bouzerar, Phys. Rev. B **94**, 094437 (2016).
[32]T. Shinjo, Y. Nakamura, and N. Shikazono, "Magnetic study of $Fe_3Si$ and $Fe_5Si_3$ by Mössbauer effect," J. Phys. Soc. Jpn. **18**, 797–801 (1963).
[33]R. Zach, J. Toboła, W. Chajec, D. Fruchart, and F. Ono, "Magnetic properties of MM'X (M = Mn, M′ = 3d or 4d metal, X = P, As, Si, Ge) compounds with hexagonal or orthorhombic crystal structure," Solid State Phenom. **194**, 98–103 (2012).
[34]L. Diallo, L. Lechevallier, A. Fnidiki, J. Juraszek, M. Viret, and A. Declémy, "Characterization of nanostructure in low dose Fe-implanted p-type 6H-SiC using atom probe tomography," J. Magn. Magn. **481**, 189–193 (2019).